Available online at www.sciencedirect.com

ScienceDirect

Energy Procedia 75 (2015) 1005 – 1020

Energy Procedia

The 7th International Conference on Applied Energy – ICAE2015

Thermo-Economic Analysis of Combined Cycle MED-TVC Desalination System

A.S.Hanafi[a] , G.M.Mostafa[a] , A.Fathy[a]* , A.Waheed[a]

[a]*Department of power mechncial engineering, Cairo university, Cairo, Egypt*

Abstract

In the present work, thermo-economic model of a superstructure combined cogeneration power plant is studied. Engineering Equation Solver "EES" code is used to study the enhancement of the thermal performance, the environmental impact and the economics cost of the plant. Optimum design point for maximum production of power and water is obtained, through developing mathematical model of separate system, and combined cogeneration system, at different operating conditions. Also, economics model, including capital cost of each unit, fuel cost, operating and maintenance cost, is developed. It is concluded that, the combined cogeneration system can save about 20.6% of Total Annual Cost "TAC" compared with separate power and water production system. The cogeneration plant consists of Gas Turbine (GT), Heat Recovery Steam Generator (HRSG), Steam Turbine (ST) and Multi Effect -Thermo Vapor Compressor Desalination System (MED-TVC).

Peer-review under responsibility of Applied Energy Innovation Institute

Keywords: Performance analysis; combined cycle; Gas turbine; HRSG; steam turbine; MED desalination.

1. Introduction

Over the last few decades, the demand on power and water has increased, due to the growth of population that leads to an increase in fuel consumption, limitations in fuel resources and lack in fresh water resources, especially in Arab gulf region. Thus, the combined cogeneration power plants becomes the most efficient solution for producing both power and water with minimum fuel consumption and increased thermal, economics and environmental performance of the plant. There are many published researches that studied thermo-economic performance of combined cogeneration power plant in order to obtain the optimum operating point for producing maximum power and water with minimum fuel consumption and cost. WU. Xainali [1] studied new cogeneration system, including coal fired thermal plants, MSF system and RO desalination system. Simplified superstructure model of the system is presented which includes all the possible alternative configuration of cogeneration system. This maturity models can make an accurate evaluation of process parameter and economic cost.Venkatarmana [2] presented a novel application of thermal energy storage TES to integrate MED system and combined cycle power plant (CCPP) for simultaneous energy conservation and water desalination. Ali Nashar [3]

* Corresponding author. Tel.: +2-0100-528-8448.
E-mail address: amrfathy.86@gmail.com.

Peer-review under responsibility of Applied Energy Innovation Institute
doi:10.1016/j.egypro.2015.07.342

developed and described superstructure model of triple hybrid power-MSF-RO system which contain the potential interaction of material streams and energy streams involved in combined system. A.Ravire [4] developed thermo-economic optimization model, that has taken into account the frequent of design operation of combined cycle gas turbine power plant with corresponding drop in efficiency. Sonjay [5] discussed rational efficiency and non-dimensional component wise exergy destruction for a cooled gas turbine based combined cycle plant. Z.Gomar [6] dealt with a techno economic analysis to select the most economical desalination method for the "Asloayeh" combined power plant. Applicable methods to generate plant make up water like RO, MED by utilizing main stack exhaust gas heat recovery and MED-TVC by employing steam extraction from HRSG LP line are investigated. Fuad Alasfour [7] performed a parametric analysis on TVC desalination system, and the study recommended that effort should be directed to achieve best setting for desalination process to minimize exergy destruction and increase gain ratio by improving design of such component. Darawish [8] has devoted his work to review the present and possibly used desalting methods, in addition to the way fuel energy passes through to supply energy needs either thermal, mechanical or both to desalter. This to point the most efficient to apply and less efficient to avoid

Many combined cogeneration power plants have been established in the last years for producing both power and water in Mega production at Gulf Region. Al-Tweelah A1, located in UAE, produces 1350 MW net power through 8 gas turbines and 3 back pressure steam turbines with 85 MIGD of distillate water from. Fourteen MED-TVC units and four MSF units with approximate 85% utilization factor (ε_u) and 15.8 Power to Water Ratio (PWR) are used. AL FUJAIRA power plant, also located in UAE, produces 2000 MW net power through 5 gas turbines and 3 condensing steam turbines with 130 MIGD distillate water through 12 MED-TVC units and 30 MIGD through RO units. In KSA; there is SHOIBA combined cogeneration power plant, which produces 862 MW net power from three gas turbines and one back pressure steam turbine with 45 MIGD of distillate water through 3 MSF units. In Qatar; RAS LUFFAN C, which produces 2730 MW through 8 gas turbines and 4 steam turbines and produces 63 MIGD distillate water through 10 MED-TVC units.

In the present work, thermo-economic performance analysis has been carried out on combined cogeneration plant. Investigation is performed to obtain the optimum operating conditions for producing both power and fresh water. The effect of different parameters on plant performance is studied. The thermal analysis on each separate component and the whole combined cogeneration power plant is also studied. The combined power plant produces 1296 MW net power through 3 gas turbines, 300 MW each and one back pressure steam turbine, which produces 396 MW and 10 MED-TVC units which produce 73.4 MIGD of distillate water with a utilization factor (ε_u) 76.5% and 17.65 PWR.

2. Mathematical modeling

2.1. Combined cogeneration cycle

The combined cogeneration power plant, studied in the present work, as shown in Fig.(1). The cycle consists of a gas turbine, a HRSG, a back pressure steam turbine and a MED-TVC units. In the gas turbine, the atmospheric air is compressed through the compressor stages to higher pressure and temperature, then it enters the combustion chamber, where it is mixed with the fuel (natural gas). After combustion process, high temperature gases enter the gas turbine to produce mechanical work. Part of this work is used to drive the compressor, while the network is used to produce electrical power through an electric generator. Instead of losing high temperature exhaust gases through the stack; the gases are fed to an unfired HRSG for producing steam to drive steam turbine. Bled steam is extracted from high and low pressure steam turbines for regenerative process through three feed water heaters. In the feed circuit of the plant, there exist one closed type feed water heater, followed by open (deaerator) feed water, and finally another closed feed water heater. The steam turbine exhaust is directed to a steam condenser at the back pressure. Alternatively, the exhausted steam is used as a motive steam in Thermo Vapour Compressor of MED-TVC unit for producing distilled water. The product distillate can be used in potable water production, irrigation system and boiler feed water (make up) …..etc

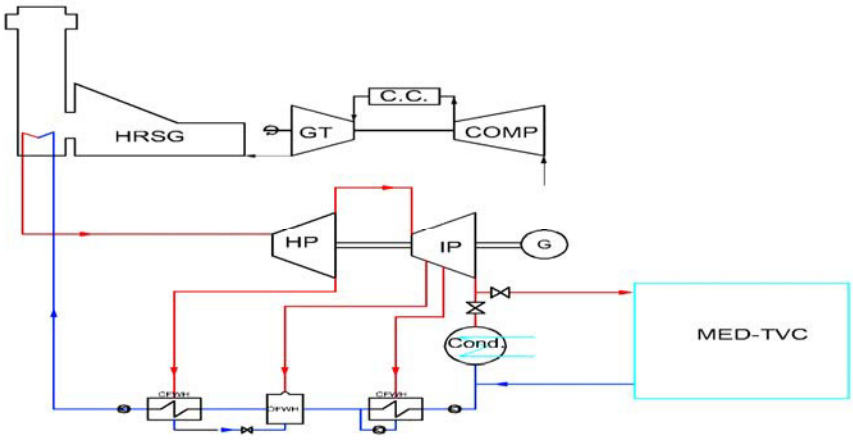

Fig. 1 Schematic diagram of a combined cogeneration power plant.

The following design procedures are used to analyze the performance of individual components of the combined cogeneration power plants; equations (1)-to-(11). The different model parameters are described in Table (1). The design equations of the combined cogeneration power plant are:

$$\dot{W}_C = \dot{m}_a C_{pa} \times (T_2 - T_1) \tag{1}$$

$$\dot{W}_T = \dot{m}_G C_{pg} \times (T_3 - T_4) \tag{2}$$

$$\dot{W}_N = \left(\dot{W}_T - \frac{\dot{W}_C}{\eta_M} \right) \times \eta_M \times \eta_G \tag{3}$$

$$\left(A/F\right)_{ACT} = \frac{\left(T_3 \times C_{pg}\right) - \left(C.V \times \eta_{CC}\right)}{\left(T_2 \times C_{pa}\right) - \left(T_3 \times C_{pg}\right)} \tag{4}$$

$$\eta_{GT} = \frac{W_N}{\dot{M}_F \times C.V} \tag{5}$$

$$\dot{m}_{ST}\left(h_{st,in} - h_{st,out}\right) = \dot{M}_G \times \left[\left(C_{pg,T_4} \times T_4\right) - \left(C_{pg,T_7} \times T_7\right) \right] \tag{6}$$

$$Q_{add,HRSG} = \dot{m}_G \times \left[\left(C_{pg\ T_{in}} \times T_{in}\right) - \left(C_{pg,T_{out}} \times T_{out}\right) \right] \tag{7}$$

$$S_{HRSG} = \frac{Q_{add,HRSG}}{U_{ovr} \times F \times \theta_{LMTD}} \tag{8}$$

$$W_S = \left(h_1 - h_2\right) + \left(1 - y_1\right) \times \left(h_2 - h_3\right) + \left(1 - y_1 - y_2\right) \times \left(h_3 - h_4\right) + \left(1 - y_1 - y_2 - y_3\right) \times \left(h_4 - h_5\right) \tag{9}$$

$$\eta_{ST} = \frac{\dot{m}_{st} W_S}{Q_{add}} \tag{10}$$

Table. 1 Model parameters for CCPP 1

Parameter	Value	Parameter	Value
Model parameters for combined cycle power plants (CCPP)			
Net power output	1297 MW	Economizer overall heat transfer coefficient	42.6 W/m2K
Pressure ratio of gas turbine cycle	17	Evaporator overall heat transfer coefficient	43.7 W/m2K
Isentropic efficiency of compressor	84%	Surperheater overall heat transfer coefficient	50 W/m2K
Isentropic efficiency of gas turbine	94%	Pinch point temperature	20°C
Air inlet temperature of compressor	298 K	Steam turbine inlet temperature	823 K
Gas turbine inlet temperature	1773 K	Steam turbine inlet pressure	110 bar
CCPP Stack Temperature	1028 K	Condenser pressure	2.8 bar
Heat exchanger gas exit temperature	525 K	Isentropic efficiency of steam turbine	90 %
Combustion chamber Efficiency	98%	Isentropic efficiency of pump	85 %
Generator Efficiency	98%	Cascade backward feed water heater pressure	40 bar
Mechanical Efficiency	99%	Open feed water heater pressure	20 bar
Theoretical air to fuel ratio	15.44	Pumped forward feed water heater pressure	10 bar
Fuel Lower calorific value NG	47141 kJ/kg	Terminal temperature difference	5°C

2.2. MED-TVC System

Fig.(2) shows a schematic diagram of one of ten typical MED-TVC units. The total rate of distillate water production is 73.4 MIGD, where each unit produces 1391 m^3/h of distillate water. D&S motive steam, from low pressure steam turbine exit at 2.8 bar, enters the TVC system. This steam is used to draw and compress entrained vapour from the last effect of the MED unit at a saturation temperature of 43°C to higher pressure and temperature. The compressed steam enters the first effect at a top brine temperature TBT 63 °C, while preheated feed water enters the first effect at temperature 53 °C. In the first effect, the compressed steam is condensed, while it heats up the feed water to the saturation temperature of the first effect. The condensed vapour is returned back to steam cycle. The generated vapour from the feed water in the first effect is partially condensed in the last preheater section, while heats up the feed water. This wet vapour, then is supplied to the second effect, as a heating steam. The brine or remaining feed water of the first effect is supplied to the second effect, as a raw water. The saturation temperature of the second effect is less than that of the first effect by ΔT_{effect}. The heating steam of the second effect is condensed and then throttled in the first flash box to extract more vapour to the next effect, before being exhausted, as a product or distillate water. The first flash box saturation temperature is less than that of the second effect by ΔT_{effect}. The vapour extracted in the first flash box is mixed with brine vapour produced from second effect to enter next effect for heating feed water. The distillate water in flash box is drawn to the next flash box until it reaches last flash box. This cycle is repeated until reaches last effect. In the last effect, part of the brine vapour formed is entrained by TVC, while the remaining brine vapour is mixed with vapour out from the last flash box and enters the condenser. The condensed vapour in the condenser is mixed with the final product. The raw sea water is heated in the condenser, and then divided to two parts. The first and major part is rejected to sea, while the second part represents the raw water that enters the preheaters. The parameters of MED-TVC are described in Table (2).

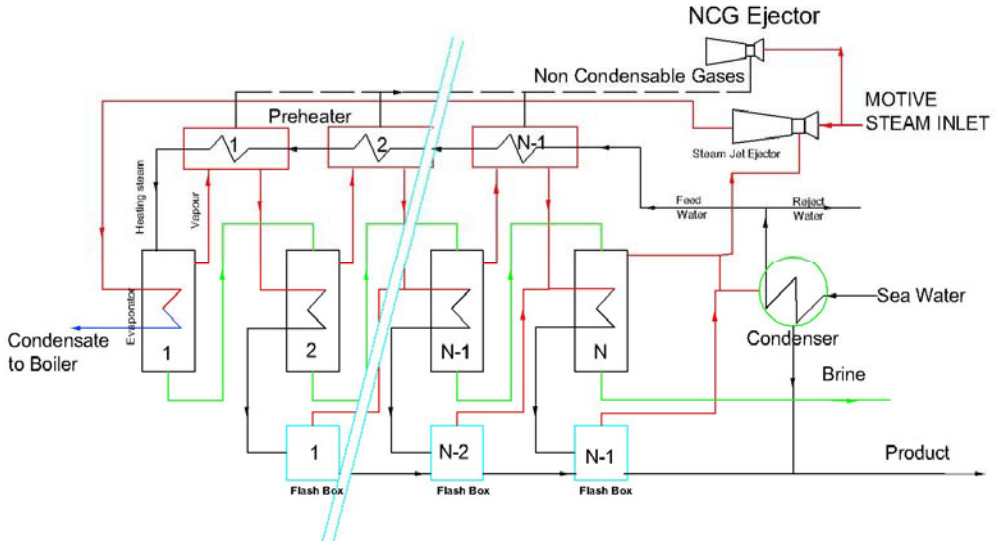

Fig. 2 Schematic diagram of MED-TVC system.

Table. 2 Model parameters for MED-TVC

Parameter	Value	Parameter	Value	Parameter	Value
N	7	ΔT_{eff} (C)	3.67	T_f (C)	53
M_d (m^3/d)	33,384.96	TBT (C)	63	T_{cw} (C)	25
X_f (ppm)	38,500	T_n (C)	43		

Thermal vapour compressor governing equations are:

$$\dot{m}_{ms}\eta_m V_0 = \left(\dot{m}_{ms} + \dot{m}_{env,n}\right)V_2 \tag{11}$$

$$\left(\dot{m}_{ms} + \dot{m}_{env,n}\right)\left(h_{ej,2} + \frac{V_2^2}{2}\right) = \dot{m}_{env,n}h_{ej,1} + \dot{m}_{ms}\left(h_{ej,0} + \frac{V_0^2}{2}\right) \tag{12}$$

$$h_{ej,3s} = h_{ej,2} + \frac{V_2^2}{2\eta_d} \tag{13}$$

$$h_{ej,3} = h_{ej,2} + \left(h_{ej,3s} - h_{ej,2}\right)/\eta_{co} \tag{14}$$

The heating steam mass flow rate to the first effect is calculated form:

$$\dot{m}_{S,1} = \dot{m}_{ms} + \dot{m}_{env,n} \tag{15}$$

Energy Balance of the i^{th} effect states that:

$$\dot{m}_{S,i}\left(h_{si,i} - h_{so,i}\right) = \left(\dot{m}_{feed,i} - M_{BV,i}\right)C_{P_{f,i}}T_{B\,i} - \dot{m}_{feed,i}C_{P_{f,i-1}}T_{f,i-1} + \dot{m}_{BV,i}h_{v,i} \tag{16}$$

Energy Balance of the i^{th} preheater results

$$\dot{m}_{BV,i}\left(h_{vi,i} - h_{vo,i}\right) = \dot{m}_{feed}C_{P_{feed}}\left(T_{fo,i} - T_{fi,i}\right) \tag{17}$$

Mass Balance and Energy Balance of i^{th} flashing Box state that:

$$\dot{m}_{S,i} = \dot{m}_{X,i} + \dot{m}_{L,i} \tag{18}$$

$$\dot{m}_{X,i} = x_i \dot{m}_{S,i} \tag{19}$$

$$\dot{m}_{S,i} h_{So,i} = \dot{m}_{X,i} h_{X,i} + \dot{m}_{L,i} h_{L,i} \tag{20}$$

Energy Balance of the bottom condenser gives:

$$\dot{m}_{S,n+1} h_{Si,n+1} = \dot{m}_{Sea} C_{P_{Sea}} \left(T_{fi,n-1} - T_{Sea} \right) + \dot{m}_{d,c} h_{d,c} \tag{21}$$

$$\dot{m}_{sea} = \dot{m}_{feed} + \dot{m}_{rej} \tag{22}$$

$$\dot{m}_{d,c} = \dot{m}_{BV,n} - \dot{m}_{env,n} + \dot{m}_{X,n} \tag{23}$$

Distillate mass flow rate is calculated from:

$$\dot{m}_d = \dot{m}_{L,n} + \dot{m}_{S,n+1} \tag{24}$$

Rejected brine mass flow rate can be found from:

$$\dot{m}_b = \dot{m}_{feed,1} - \sum_{i=1}^{n} \left(\dot{m}_{BV,i} \right) \tag{25}$$

First effect heat transfer surface area is estimated from:

$$A_1 = \frac{\dot{m}_{d,1} h_{fg,1}}{U_1 \left(T_{s,i} - TBT \right)} \tag{26}$$

Heat transfer surface area in for the 2nd to nth effects can be estimated from:

$$A_i = \frac{\dot{m}_{d,i} \left(h_{si,i} - h_{so,i} \right)}{U_1 \Delta T_{eff,i}} \tag{27}$$

The bottom condenser heat transfer surface area can be found from:

$$A_C = \frac{\dot{m}_d h_{fg,c}}{U_c \theta_{LMTD}} \tag{28}$$

3. Results and Discussion

3.1. Gas turbine performance

Fig.(3.A) indicates the effect of nominal pressure ratio (PR_n) on the gas turbine specific work. It is noticed that, the specific turbine work increases by increasing the nominal pressure ratio (PR_n) until it reach optimum point, after which, any further increase in the pressure ratio will cause a decrease in the net specific work. This may be attributed to the high increase in the compressor work w.r.t the small increase in the turbine work. On the other hand, increasing the maximum cycle temperature (T_3), will lead to increase in net specific work due to the increase in the work of turbine.

Fig.(3.B) shows the dependence of the gas turbine thermal efficiency (η_{GT}) on the nominal pressure ratio (PR_n). As can be seen from this figure, (η_{GT}) increases by increasing nominal pressure ratio PRn. This is referred to, increasing nominal pressure ratio PRn will increase temperature of air at compressor exit (T_2), and with constant maximum cycle temperature (T_3) will lead to decrease in the amount of fuel mass flow rate ($\dot{m}_f$), needed for heat addition at constant gas turbine power. At the same time, increasing of maximum cycle temperature (T_3) has small significant effect on the thermal efficiency, due to increase the fuel consumption and the work of gas turbine together.

The effect of nominal pressure ratio (PR_n) and maximum cycle temperature (T_3) on exhaust gases flow rate and temperature is significant for cogeneration. Fig.(3.C) shows that, at constant gas turbine power, the mass flow rate of exhaust gases ($\dot{m}_g$) decreases sharply with the increase of nominal pressure ratio (PR_n) until it reaches its lowest value, after which further increase in nominal pressure ratio (PR_n) slightly leads to an increase in ($\dot{m}_g$). This takes place due to the inverse relation between the exhaust gases mass flow rate ($\dot{m}_g$) and the specific gas turbine work (W_n) to maintain constant power output. Similarly, increasing maximum cycle temperature causes a decrease in ($\dot{m}_g$), due to the increased specific gas turbine work at constant power output.

On the other hand, Fig.(3.D) shows that increasing nominal pressure ratio (PR_n) at constant maximum cycle temperature (T_3), leads to a decrease in the exhaust gases temperature (T_4) due to the increase of the work of turbine. However, increasing (T_3) will lead to an increase in exhaust gas temperature (T_4).

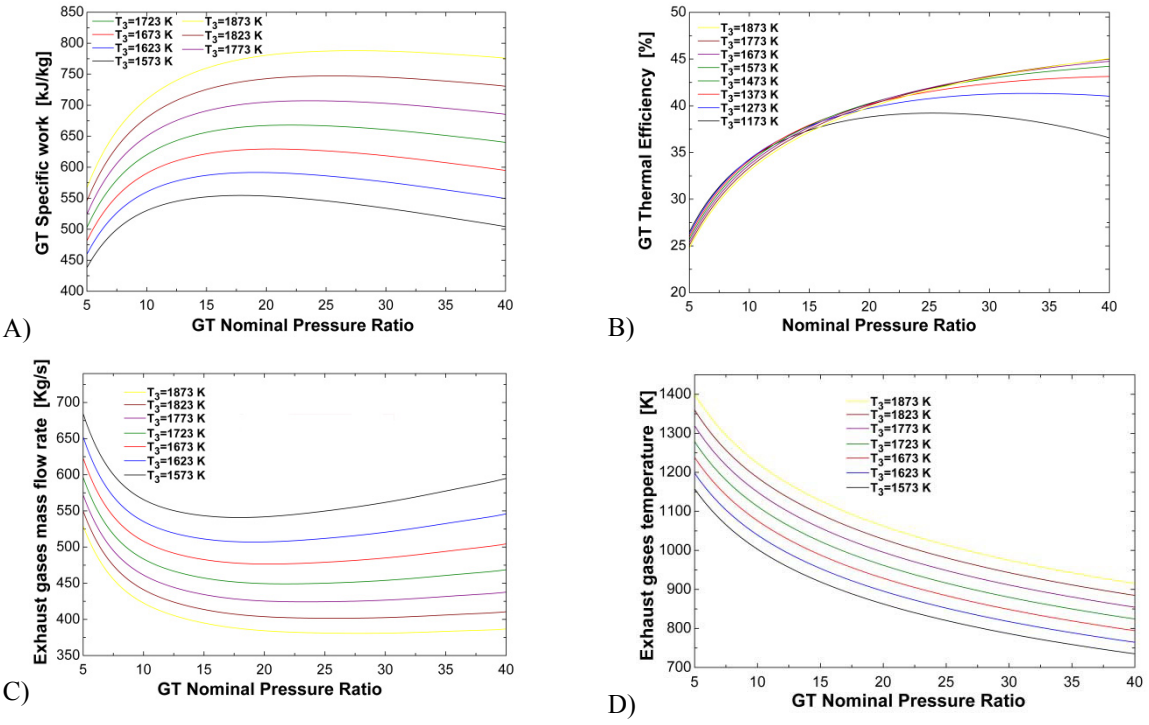

Fig. 3 Gas turbine perform-ance curves.

3.2. Heat recovery steam generator (HRSG) performance

The effect of gas turbine parameters on HRSG performance is illustrated in Fig.(4). Fig.(4.A) indicates that increasing nominal pressure ratio (PR_n), leads to a sharp decrease in steam mass flow rate ($\dot{m}_{st}$) until the nominal pressure ratio (PR_n) reaches 15. This is attributed to the significant decrease in exhaust gases temperature (T_4) of gas turbine. If the nominal pressure ratio (PR_n) is further increased,

steam mass flow rate ($\dot{m}_{st}$) decreases with lower rate according to the associated increase of exhaust gas mass flow rate ($\dot{m}_g$). Fig.(4.B) shows the effect of changing the pinch point temperature (PPT) on steam mass flow rate ($\dot{m}_{st}$) at constant gas and steam conditions. It can be noticed that, steam mass flow rate ($\dot{m}_{st}$) decreases gradually with increasing the pinch point temperature (PPT). This may be referred to the increased latent heat of steam as the PPT increases. Due to the rate of heat transfer between exhaust gases and water is decreased by increasing PPT that decreases steam mass flow rate ($\dot{m}_{st}$). Fig.(4.C) shows the effect of the generated steam temperature and pressure on its mass flow rate. It is evident that, the increase of steam temperature will lead to a decrease in steam mass flow rate ($\dot{m}_{st}$), due to the increase in the degree of superheat at constant heat gain. However, increasing boiler pressure will cause a decrease in the heat required for the evaporator, because the decrease in latent heat, consequently, leads to an increase in steam mass flow rate ($\dot{m}_{st}$).

3.3. Steam turbine performance

The effect of changing boiler pressure on steam turbine thermal efficiency is indicated in Fig.(5). It can be seen that, increasing the boiler pressure, causes an increase in the steam turbine work, which in turn increases the thermal efficiency of steam turbine (η_{st}). On the other hand, increasing the generated steam temperature leads to an increase in the degree of super heat and work of steam turbine, which gradually increases thermal efficiency of steam turbine (η_{st}). The incomplete curve of Fig.(5) indicates the high pressure limit at which the steam exits from the high pressure turbine with a high moisture content that affects the turbine performance and damages the blades of the low pressure turbine.

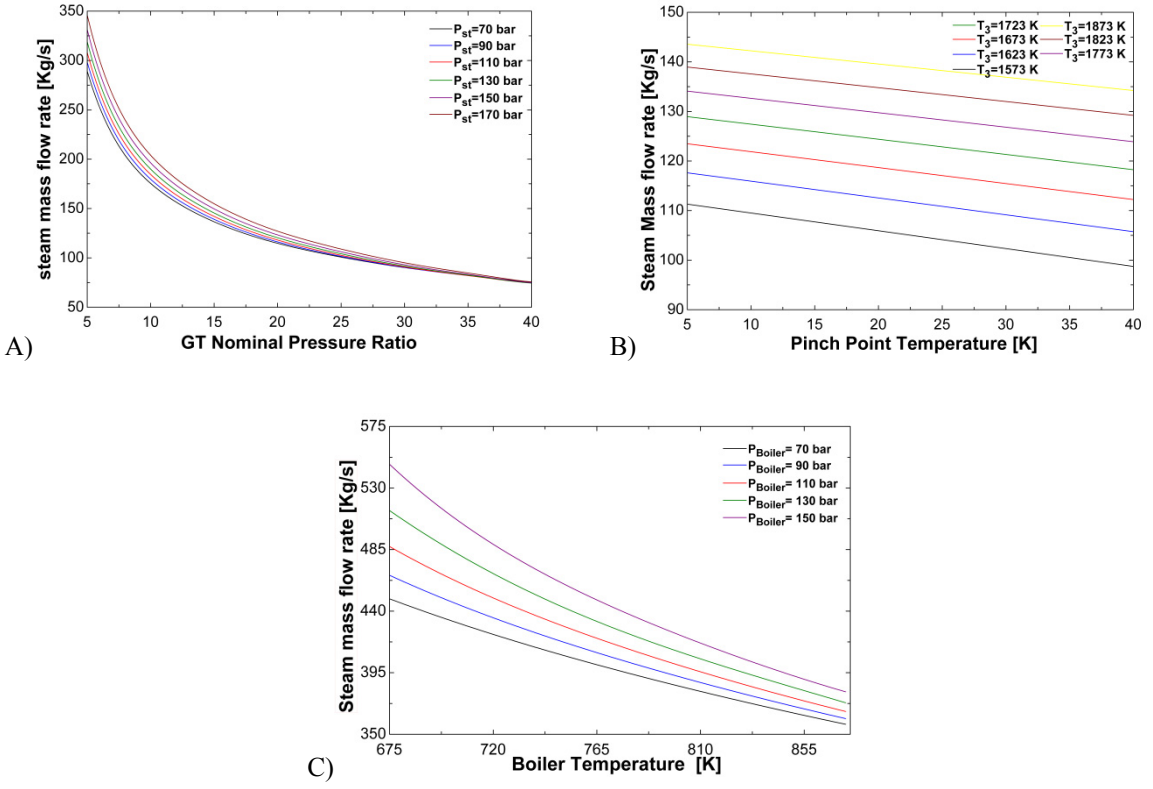

Fig. 4 HRSG performance curves.

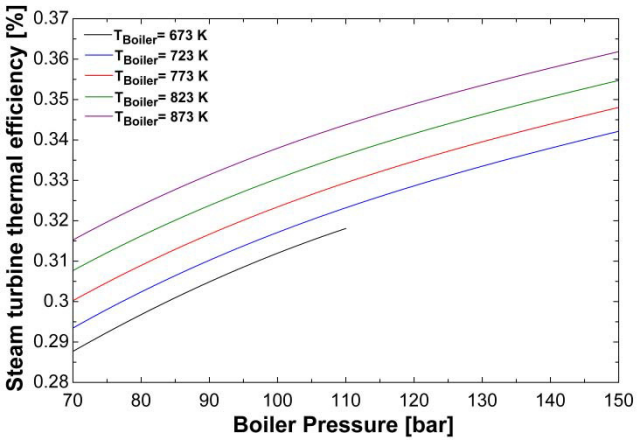

Fig. 5 Effect of steam boiler pressure on steam turbine thermal efficiency.

3.4. MED-TVC performance

The performance curves of the MED-TVC system are shown in Fig.(6). It is clear that, increasing the number of effects (*N*), increases performance ratio (*PR*) of MED-TVC, due to the increase in the total distillate mass flow rate ($\dot{m}_d$). On the other hand, increasing the top brine temperature (TBT), leads to an increase in the energy needed for evaporation per effect which decreases both the distillate mass flow rate ($\dot{m}_d$) and performance ratio (*PR*). It can be observed also that, increasing the compression ratio (*CR*) of thermo compressor (the ratio between compressed steam exits from TVC to the pressure of entrained vapour at constant motive steam pressure, increases the required mass flow rate of motive steam ($\dot{m}_{mst}$), due to the increased discharge pressure of mixed steam out from thermocompressor. Inversely, increasing the pressure of the motive steam at constant compression ratio (*CR*), decreases motive steam mass flow rate ($\dot{m}_{mst}$), at constant discharge pressure of mixed steam which increases entrainment ratio accordingly. It is also evident that, increasing the last effect temperature (T_n), causes a decrease in the total production of distillate mass flow rate ($\dot{m}_d$) and a slightly decrease in performance ratio (*PR*), due to the decreasing in the mass flow rate of motive steam ($\dot{m}_{mst}$). It can also be concluded that, the heat transfer surface area of all effects decreases with increasing top brine temperature (TBT). This may be attributed to that, with a high top brine temperature (TBT), distillate mass flow rate ($\dot{m}_d$) decreases and overall temperature differences increase.

3.5. Combined Cogeneration

The effect of changing the gas turbine parameters on the combined cycle performance is indicated in figures (7), (8) and (9). As shown in Fig.(7), increasing gas turbine power leads to an increase in both distillate mass flow rate ($\dot{m}_d$) and steam turbine power. This may be referred to; increasing gas turbine power will increase exhaust gas mass flow rate ($\dot{m}_g$), and hence will increase the steam mass flow rate ($\dot{m}_{st}$), which will lead to an increase in steam turbine power and production of distillate water. Thus no heat is rejected from this plant as waste heat. In other words, all the energy transferred to the steam in the boiler is utilized as either process heat or electric power. Thus it is appropriate to define a utilization factor (ε_u) for a cogeneration plant as:

$$\varepsilon_u = \frac{Net\ work\ \text{output} + \text{Process heat delivered}}{Total\ \text{heat input}}$$

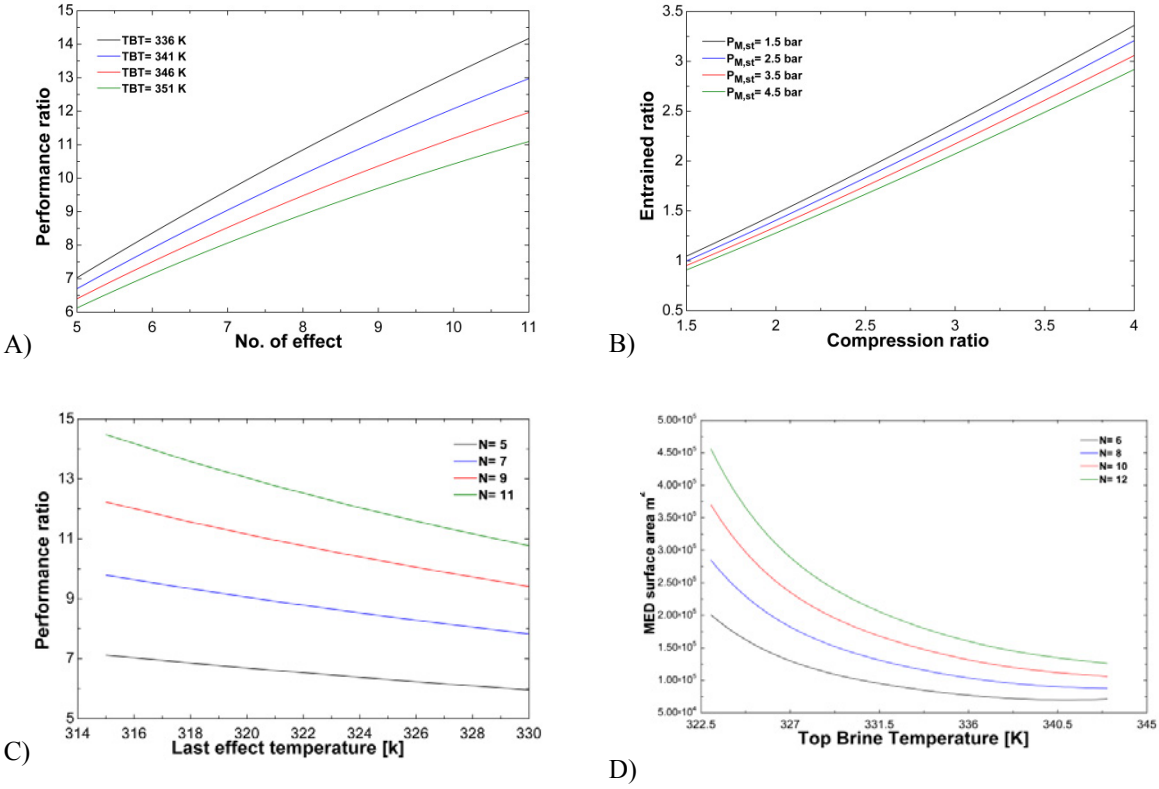

Fig. 6 MED-TVC system performance curves.

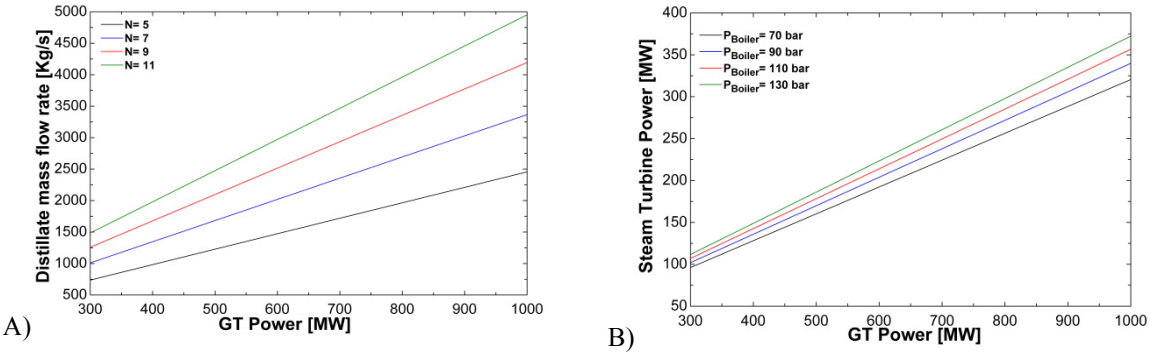

Fig. 7 Effect of gas turbine output power on steam turbine power and distillate mass flow rate

Fig.(8) shows the effect of changing the nominal pressure ratio (PR_n) of gas turbine on distillate mass flow rate ($\dot{m}_d$). It can be seen in Fig.(8-A) that, increasing nominal pressure ratio (PR_n) causes a decrease in the distillate mass flow rate ($\dot{m}_d$), where, as concluded earlier increasing nominal pressure ratio (PR_n) decreases the steam mass flow rate ($\dot{m}_{st}$), and hence the distillate mass flow rate ($\dot{m}_d$). The effect of the

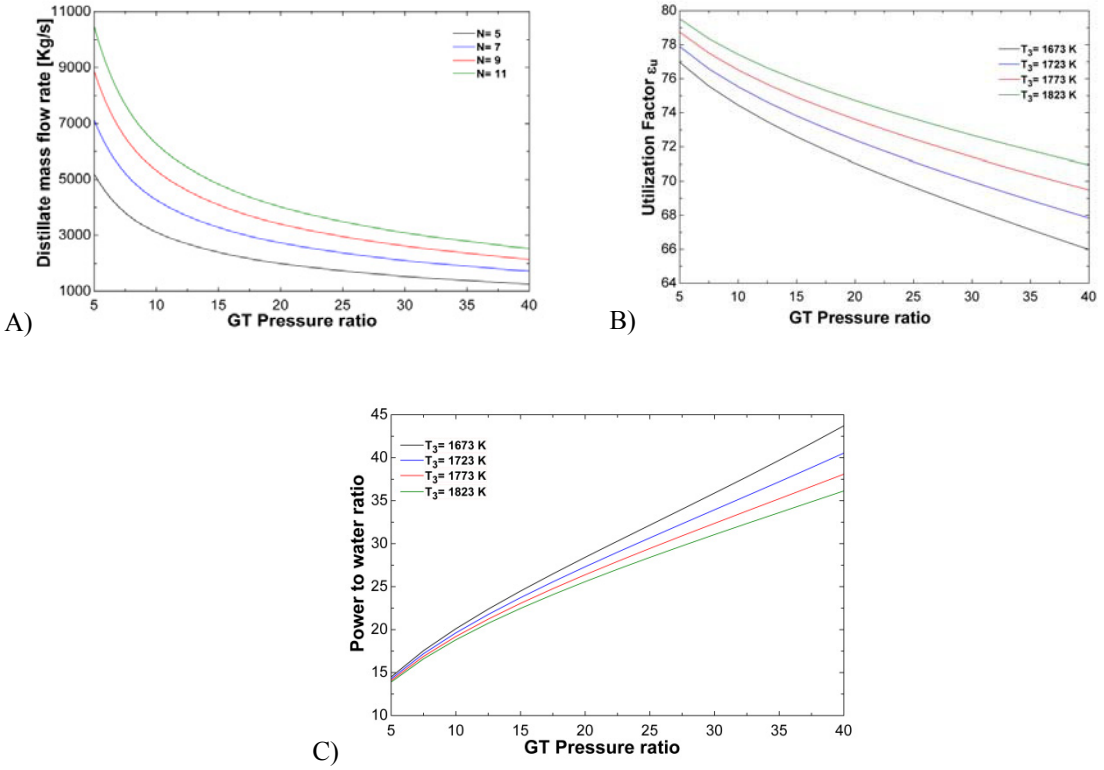

Fig. 8 Effect of gas turbine pressure ratio on cogeneration cycle performance.

nominal pressure ratio (PR_n) on the utilization factor (ε_u) of the cogeneration cycle is indicated in Fig.(8-B). In the cogeneration plant, the heat energy used in desalination is added to the term of power gained, nominal pressure ratio (PR_n) has a complex effect on the plant because increasing nominal pressure ratio (PR_n), increases the specific net work of gas turbine. However, exhaust gas mass flow rate ($\dot{m}_g$) and exhaust gas temperature (T_4) decrease which leads to a decrease in both steam turbine power and distillate mass flow rate ($\dot{m}_d$). Accordingly utilization factor (ε_u) of the cogeneration cycle decreases as the nominal pressure ratio (PR_n) increases. On other hand, increasing the maximum cycle temperature (T_3) causes an increase in (ε_u), due to the increase of exhaust gas temperature (T_4) and steam mass flow rate ($\dot{m}_{st}$). This, in turn, increases both steam turbine power and distillate mass flow rate ($\dot{m}_d$). Fig.(8-C) shows the power to water ratio (PWR) versus the nominal pressure ratio (PR_n) of gas turbine. As shown in this figure, increasing nominal pressure ratio (PR_n) of gas turbine will increase power to water ratio (PWR), i.e. nominal pressure ratio (PR_n) has better effect in producing power than water. The same effect applies to the maximum cycle temperature (T_3).

Fig.(9) Shows the gas turbine power effect on exhaust gas mass flow rate ($\dot{m}_g$), steam mass flow rate ($\dot{m}_{st}$) and distillate mass flow rate ($\dot{m}_d$). As shown in this figure, changing gas turbine power has significant proportional effect on both gas and distillate flow rates and almost no effect on steam mass flow rate.

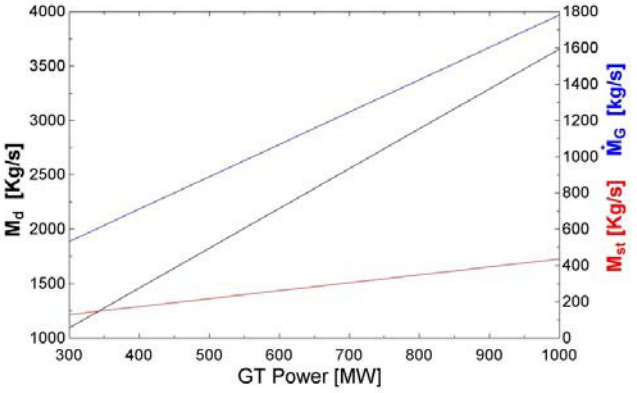

Fig. 9 Effect of GT power on mass flow rates of exhaust gases, steam and distillate water.

4. Economic study

Economic analysis plays an essential rule in the evaluation of power plant performance and reliability. Moreover, economic analysis illustrates the effect of improving thermal performance on the cost of power and water production due to cogeneration. Comparison is performed on the total annual cost bases. The total annual cost (TAC) of the power plant includes capital cost, fuel cost and O&M cost per year for combined cogeneration. This TAC is compared with that including separate production of power and water. The total annual cost is calculated from:

$$TAC = C_i (AFCR) + C_f + C_{O\&M} \tag{29}$$

Where :

TAC	:	Total annual cost, in ($/year).
C_i	:	Capital investment, in ($).
$(AFCR)$	:	Annual fixed charge rate, in percentage, calculated from table (3) [9].
C_f	:	Annual fuel cost, in ($/year).
$C_{O\&M}$	:	Annual O&M cost, in ($/year).

Table (3) indicates the annual fixed charge rates (AFCR) and table (4) illustrates the power and water costs for a combined cycle power plant integrated with MED-TVC. Capital investment is the summation of combined cycle and MED-TVC costs and is given by:

$$C_i = C_{combined} + C_{MED-TVC} \tag{30}$$

Fuel cost for cogeneration can be calculated from:

$$C_f = P_{cog} \times OP \times NHR_{GT} \times F_p \tag{31}$$

Where :

P_{cog}	:	Cogeneration plant generated power, in kW
HOP	:	Hours of operation for the cogeneration plant
NHR_{GT}	:	Net Heat Rate of gas turbine
F_p	:	Fuel price in ($/year).

Table. 3 Annual fixed charge rate

Charge Rate	Percent %
Return	7.7
Depreciation	1.4
Taxes	6.5
Insurance	0.4
Total	16.0

Table. 4 Estimated component costs for MED-TVC with combined cycle power plant

Description	Cost
Combined cycle capital cost	917 $/KW
MED-TVC capital cost	1,524 $/m^3/d
Separate steam boiler	100,000 $/T/hr
Natural gas price F_P	4.8 $/MBTU
Fixed O&M$_{combined}$ cost	13.17 $/KW.year
Variable O&M$_{combined}$ cost	3.6 $/MW.h
Fixed O&M$_{MED-TVC}$ cost	0.39 $/m^3

The electric power and water consumption prices per year is estimated, based on unit price in Gulf area [10] as, (C_e = 0.07 $/kWh) and (C_w = 2.5 $/m^3) for power and water, respectively. On the other hand, the fuel cost for separate combined cycle and MED-TVC unit is:

$$C_f = P_{cog} \cdot OP \cdot NHR_{GT} \cdot F_p + \frac{M_{ms} \Delta h \, HOP \, F_P}{\eta_{SB}} \quad (32)$$

Where : M_{ms} : Motive steam mass flow for MED-TVC
Δh : The change of enthalpy gain for steam
η_{SB} : Efficiency of separate boiler

The net cash flow income per year ($C_{f,net}$) and the income cash flow ($C_{f,i}$) are expressed by :

$$C_{f,net} = C_{f,i} - TAC \ (\$/year) \quad (33)$$

$$C_{f,i} = (C_e \cdot P) + (C_w \times M_d) \ (\$/year) \quad (34)$$

The Payback Period is the time required to recover the cost of an investment and is calculated from:

$$PB = C_i(investment) / C_{f,i}(cashflow \ per \ year) \quad (35)$$

Fig. (10) Shows a comparison between the total annual costs (TAC), capital investment and net cash flow of cogeneration power plant and those of separate combined cycle and MED-TVC units. It can be seen that, total annual costs (TAC) for combined power plant and MED-TVC separate units is higher by 20.6% than total annual costs (TAC) of combined cogeneration system. This may be attributed to addition of initial and fuel consumption costs for separate boiler of MED-TVC to the total annual cost. It can be concluded also that, the total annual cost for separate power and water production is $937,287,772.00, and the net cash flow from it is $162,669,480 with payback period of twenty months. On the other hand, cogeneration power plant total annual cost is $744,257,540.00, and its net cash flow is $355,700,072.00, with payback period of eighteen months. It might noticed that, the combined cogeneration power plant integrated with desalination system is more profitable than other gas turbine based dual purpose power and desalination plants [11]. At the same time, the integrated configurations (cogeneration) are proven to be more thermodynamically efficient and economically feasible than single purpose power generation and water production plants[12].

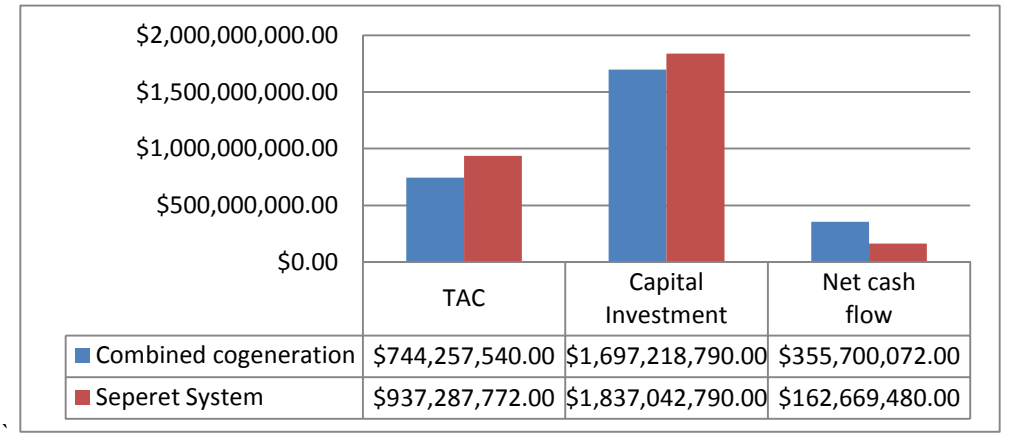

Fig. 10 Comparison of TAC, capital investment and net cash flow for the optimized cogeneration systems and other two separate production systems

5. Conclusions

In the present work, thermo-economic analytical study of combined cogeneration power plant for power and water production is performed using Engineering Equation Solver EES software. Many operating conditions were studied, in order to obtain the optimum point for maximum production of water and power with best overall efficiency. This study shows that the best utilization factor can be obtained from combined cogeneration cycle which reaches above 80% [13], that can save more than 30% of thermal efficiency comparing to combined cycle. The study shows that, maximum cycle temperature (T_3), nominal pressure ratio (PR_n) and exhaust gas mass flow rate ($\dot{m}_g$) are the main factors controlling power and water production and performance of plant. Compared with the separate system, combined cogeneration system is more economical and reduces production cost of power and water by saving about 20.6% of TAC and increase annual net cash flow by 118%. All subsystems used in this study have been widely used worldwide which indicate that this design method is effective.

6. Acknowledgment

The authors acknowledge the support provided by Ahmed Waheed who has a many contributions in this paper.

Nomenclature

Symbol	
A	Area of effect, m^2
A_1	Area of first effect, m^2
A_c	Area of MED condenser, m^2
A/F_{act}	Actual air to fuel ratio
C_{pa}	specific heat of air at constant pressure, kJ/kg.K
C_{pf}	specific heat of feed water at constant volume, kJ/kg.K
C_{pg}	specific heat of gas at constant pressure, kJ/kg.K
CV	Lower calorific value
f	Fouling factor
h_1	Enthalpy of steam out from HRSG, kJ/kg
h_2	Enthalpy of steam out from high pressure steam turbine, kJ/kg
h_3	Enthalpy of steam extraction enter open FWH, kJ/kg

h_4	Enthalpy of steam extraction enter low pressure FWH, kJ/kg
h_5	Enthalpy of steam out from low pressure steam turbine, kJ/kg
$h_{ej,o}$	Enthalpy of motive steam enter ejector, kJ/kg
$h_{ej,1}$	Enthalpy of entrained vapour enter ejector, kJ/kg
$h_{ej.2}$	Enthalpy of mixed steam in ejector, kJ/kg
$h_{ej,3}$	Enthalpy of compressed steam out from ejector, kJ/kg
$h_{ej.3s}$	Isentropic enthalpy of compressed steam out from ejector, kJ/kg
h_{dc}	Enthalpy of distillate leave MED condenser, kJ/kg
h_{si}	Enthalpy of steam enter MED effect, kJ/kg
h_{so}	Enthalpy of steam leave MED effect, kJ/kg
h_{vi}	Enthalpy of brine vapour enter MED preheater, kJ/kg
h_{vo}	Enthalpy of brine vapour leave MED preheater, kJ/kg
$\dot{m}_{bv}$	Brine vapour mass flow rate, kg/s
$\dot{m}_{dc}$	Distillate mass flow rate leave condenser, kg/s
$\dot{m}_{env}$	Entrained vapour mass flow rate, kg/s
$\dot{m}^f$	Fuel mass flow rate, kg/s
$\dot{m}_{feed}$	Feed water mass flow rate, kg/s
m^g	Exhaust gases mass flow rate, kg/s
$\dot{m}_l$	Distillate water mass flow rate exit from flash box, kg/s
$\dot{m}_{ms}$	Motive steam mass flow rate, kg/s
$\dot{m}_{rej}$	Rejected sea water mass flow rate, kg/s
$\dot{m}_s$	Steam mass flow rate enter MED effect, kg/s
$\dot{m}_{s1}$	Steam mass flow rate enter MED first effect, kg/s
$\dot{m}_{sea}$	Sea water mass flow rate, kg/s
$\dot{m}_{st}$	Steam mass flow rate out from HRSG, kg/s
$\dot{m}_x$	Vapour mass flow rate exit from flash box, kg/s
N	Total number of MED effects
P	Gas turbine power, KW
P_{tot}	Total power of combined cycle, KW
PPT	Pinch point temperature, K
PR_n	Nominal pressure ratio of GT
S	HRSG cross section area, m^2
T_1	Ambient air temperature enter compressor, K
T_2	Compressed air temperature leave compressor, K
T_3	Gases temperature enter turbine, K
T_4	Gases temperature leave turbine, K
T_7	Gases temperature leave HRSG, K
T_b	Brine temperature, K
T_f	Feed water temperature, K
T_{sea}	Sea water temperature, K
TBT	Top brine temperature, K
U	Overall heat transfer coefficient, W/m^2K
V	Velocity, m/s
W_c	Specific compressor work, kJ/Kg
W_n	Specific net work, kJ/Kg
W_T	Specific turbine work, kJ/Kg
X	Steam quality, %
Y	Steam extraction percentage

η_{cc}	Combustion chamber efficiency, %
η_{d}	Diffuser isentropic efficiency, %
η_{g}	Generator efficiency, %
η_{GT}	Gas turbine thermal efficiency, %
η_{mech}	Mechanical efficiency, %
η_{m}	Mixing efficiency inside ejector, %
η_{ST}	Steam turbine thermal efficiency, %
$\eta_{overall}$	Overall thermal efficiency, %
ΔT_{eff}	Temperature difference per effect, K
Subscripts	
I	number of MED effect
N	MED last effect

References

1. WU, X., et al., *Model and Design of Cogeneration System for Different Demands of Desalination Water, Heat and Power Production.* Chinese Journal of Chemical Engineering, 2014. **22**(3): p. 330-338.
2. Gadhamshetty, V., V.G. Gude, and N. Nirmalakhandan, *Thermal energy storage system for energy conservation and water desalination in power plants.* Energy, 2014. **66**: p. 938-949.
3. El-Nashar, A.M., *Cogeneration for power and desalination—state of the art review.* Desalination, 2001. **134**(1): p. 7-28.
4. Rovira, A., et al., *Thermoeconomic optimisation of heat recovery steam generators of combined cycle gas turbine power plants considering off-design operation.* Energy Conversion and Management, 2011. **52**(4): p. 1840-1849.
5. Sanjay, *Investigation of effect of variation of cycle parameters on thermodynamic performance of gas-steam combined cycle.* Energy, 2011. **36**(1): p. 157-167.
6. Gomar, Z., H. Heidary, and M. Davoudi, *Techno-Economics Study to Select Optimum Desalination Plant for Asalouyeh Combined Cycle Power Plant in Iran.*
7. Alasfour, F.N. and H.F. Alajmi, *INTEGRATION OF TVC DESALINATION SYSTEM WITH COGENERATION PLANT: PARAMETRIC STUDY.*
8. Darwish, M.A., N. Al-Najem, and N. Lior. *Towards Sustainable Energy in Seawater Desalting in the Gulf Area*. 2006.
9. Shaalan, H.E., *Generation of electric power.* Handbook of electric power calculation, 3rd ed. McGraw-Hill, 2003.
10. Saif, O., *The Future Outlook of Desalination in the Gulf.*
11. Rensonnet, T., J. Uche, and L. Serra, *Simulation and thermoeconomic analysis of different configurations of gas turbine (GT)-based dual-purpose power and desalination plants (DPPDP) and hybrid plants (HP).* Energy, 2007. **32**(6): p. 1012-1023.
12. Hamed, O.A., H.A. Al-Washmi, and H.A. Al-Otaibi, *Thermoeconomic analysis of a power/water cogeneration plant.* Energy, 2006. **31**(14): p. 2699-2709.
13. Rice, I.G., *The Combined Reheat Gas Turbine/Steam Turbine Cycle: Part II—The LM 5000 Gas Generator Applied to the Combined Reheat Gas Turbine/Steam Turbine Cycle.* Journal of Engineering for Gas Turbines and Power, 1980. **102**(1): p. 42-49.

Biography

Amr Fathy is a current research assistant in Cairo University. He works on two research topics; the first involves a Thermo-economic analysis of combined cycle MED-TVC desalination system, and the second involves one dimensional mathematical modeling and CFD investigation for steam jet ejectors. Fathy has been graduated from Mechanical power engineering department, Cairo University in 2009 and finished his master courses of Fluid Mechanics in 2011 of GPA 3.42. He currently works for National Gas Company (NATGAS) as a senior testing and commissioning engineer. He has received many trainings in the engineering field such as o Radiographic Test (RT) Level II, American Society for Non-destructive test (ASNT) , Ultrasonic Test (UT) Level II, American Society for Non-destructive test (ASNT), Visual Inspection Test (VT) Level II, American Society for Non-destructive test (ASNT) and HSE MS Workshop at Shell Egypt.